Research Paper
Computational Methods for Differential Equations
http://cmde.tabrizu.ac.ir
Vol. 14, No. 3, 2026, pp. 1230-1249
DOI:10.22034/cmde.2025.63398.2828

Robust finite difference schemes for one-dimensional parabolic singularly perturbed problems with regular layers

Kishun Kumar Sah* **and Subramaniam Gowrisankar**
Department of Mathematics, National Institute of Technology Patna, India.

Abstract

In this article, we study the midpoint finite difference scheme for the singularly perturbed parabolic convection diffusion problem on non-uniform meshes, which are determined by a generating function with the boundary layer on the right side of the domain. The non-uniform meshes considered in this work are the classical Shishkin meshes, Shishkin-Bakhvalov meshes, and Shishkin-Bakhvalov modified meshes. Uniform convergence is established with respect to the perturbation parameter on the non-uniform meshes. The backward Euler scheme is applied in the time direction and midpoint finite schemes in the space. Uniform convergence of up to second order in the space and first order in time is obtained. Two numerical examples are considered to validate the numerical and theoretical results obtained.

Keywords. Singularly perturbed parabolic problem, Regular boundary layer, Midpoint finite difference scheme, Shishkin mesh, Shishkin-Bakhvalov mesh, Shishkin-Bakhvalov modified mesh, Generating function, Uniform convergence.

2010 Mathematics Subject Classification. AMS 65M06, AMS 65M12, AMS 65M15.

1. Introduction

A singular perturbation problem in the context of parabolic equations typically involves a parameter ε multiplying the highest-order derivative term. This parameter ε is small, leading to two distinct time scales in the problem: a fast scale governed by the ε-affected terms and a slow scale where these terms are negligible. As a result, the solution exhibits behaviour that rapidly adjusts on the fast scale and slowly evolves on the slow scale. Consider a simple example, the one-dimensional heat equation with a small parameter ε

$$\frac{\partial u}{\partial t} = \varepsilon \frac{\partial^2 u}{\partial x^2}, \quad 0 < x < 1, \quad t > 0.$$

Subject to suitable boundary conditions and initial conditions, this equation describes the evolution of temperature $u(x, t)$ in a one-dimensional rod. The parameter ε reflects the relative importance of the time derivative compared to the spatial derivative. When ε is small, the solution undergoes rapid changes in the spatial direction and slower changes in time. Analyzing such problems typically involves identifying the boundary and initial layers where the solution transitions between the fast and slow scales. Techniques like matched asymptotic expansions or multiple scales are often used to systematically analyze the behaviour of solutions in these regimes. Singularly perturbed parabolic convection-diffusion problems frequently emerge across various engineering and applied mathematical domains. Illustrative instances encompass the simulation of transient viscous flow issues with high Reynolds numbers, and convective heat transfer predicaments with significant Peclet numbers. Such quandaries are delineated by partial differential equations (PDEs), wherein the foremost spatial derivative is scaled by a diminutive parameter ε.

Classical numerical methods, such as standard finite difference or finite element schemes, often yield inaccurate results when applied to problems with boundary layers using uniform meshes. Through meticulous numerical experiments, it has been observed that these classical methods typically fail to reduce the maximum point-wise error as

Received: 08 September 2024; Accepted: 05 May 2025.
* Corresponding author. Email: kishuns.phd20.ma@nitp.ac.in.

the mesh is refined, unless both the mesh parameter and the perturbation parameter ε are of comparable magnitude. Consequently, achieving precise numerical solutions using classical methods necessitates an unacceptably large number of mesh points, which depend on ε. This limitation has prompted the development of ε-uniform numerical methods, where the convergence rate and error constant remain independent of the singular perturbation parameter ε.

In recent decades, numerous researchers have devoted their efforts to developing ε-uniform numerical methods for both stationary and non-stationary problems. A wealth of literature, including books [7, 14, 20] and papers [12, 22], documents these advancements. Notably, the fitted mesh method has emerged as a prominent solution. This method employs a specialized piecewise-uniform mesh that is concentrated around boundary layers, offering a recognized strategy to overcome the constraints inherent in classical methods. Several researchers have proposed various computational approaches for solving the problem of singular perturbation subject to the problem described in Equation (2.1), considering both initial and boundary conditions. These methodologies are detailed in [1–3, 5, 10, 19, 21, 24]. In [27], the author introduced two nonstandard finite difference schemes for approximating the solution of a mathematical model of HIV infection. The technique of non-local approximation and renormalization of the denominator of the discrete derivative was employed. In [15], the author investigates isotropic finite difference discretizations of the two-dimensional (2D) and three-dimensional (3D) Laplacian operators.

In 2023, the author introduced a significant time delay two-parameter singularly perturbed one-dimensional parabolic problem within a rectangular domain, as documented in [26]. The utilization of the central finite difference method, as discussed in [9], along with the application of the Crank-Nicolson method for discretizing the time derivative on a uniform mesh, is detailed in [6]. In 2024, the author introduced ε-uniform convergence with various schemes on different meshes to address both delay and non-delay singular perturbation parabolic problems. This development is discussed in detail in reference [11, 17, 25] .

In this paper, we examine a convection-diffusion problem with time dependence in a single spatial dimension. We develop a numerical approach that combines backward Euler discretization and a midpoint upwind finite difference operator applied to classical Shishkin meshes, Shishkin-Bakhvalov meshes, and Shishkin-Bakhvalov modified meshes, which is obtained by generating functions. The presented method demonstrates first-order accuracy in the time dimension and nearly second-order accuracy in the spatial dimension. Through our analysis, we establish that the numerical solution produced by this method uniformly converges to the solution of the continuous problem concerning the singular perturbation parameter.

The paper's contents are outlined as follows. Section 2 provides an overview of the continuous problem, its reduced form, classical bounds on the solution, and its derivatives. Moving on to section 3, the discretization in the temporal direction is detailed through the application of the Euler implicit method. The proposed method's time direction is scrutinized, yielding both local and global error estimates. In section 4, achieving $\varepsilon-$uniform convergence involves obtaining more precise bounds on the solution and its derivatives. This is accomplished by decomposing the solution into distinct smooth and singular components. Section 5 introduces a numerical method featuring a discrete operator on a classical Shishkin meshes, Shishkin-Bakhvalov meshes, and Shishkin-Bakhvalov modified meshes. Section 6 establishes the satisfaction of the discrete maximum principle by the discrete operator. Numerical result and conclusion in sections 7 and 8. The numerical solution is further analysed by decomposing it into smooth and singular components, with separate error estimates for each. Demonstrating $\varepsilon-$ uniform convergence of the numerical solution, generated by the proposed method, to the continuous problem's solution is presented. The concluding section encompasses numerical experiments validating the theoretical predictions.

2. Continuous problem

Consider the singularly perturbed initial-boundary value problem

$$\begin{cases} \dfrac{\partial y(r,\theta)}{\partial \theta} + \mathfrak{L}_\varepsilon y = f(r,\theta), \quad (r,\theta) \in G \equiv \Upsilon_r \times \Upsilon_\theta, \quad \text{where} \quad \Upsilon_r = (0,1) \quad \text{and} \quad \Upsilon_\theta = (0,\mathfrak{T}], \\ y(r,0) = y_0(r) \quad \text{for} \quad 0 \le r \le 1, \\ y(0,\theta) = 0 \quad \text{for} \quad 0 < \theta \le \mathfrak{T}, \\ y(1,\theta) = 0 \quad \text{for} \quad 0 < \theta \le \mathfrak{T}, \end{cases} \tag{2.1}$$

where,

$$\mathfrak{L}_\varepsilon y(r,\theta) \equiv -\varepsilon \frac{\partial^2 y(r,\theta)}{\partial r^2} + \Psi(r)\frac{\partial y(r,\theta)}{\partial r} + \Phi(r,\theta)y(r,\theta),$$

with $\Psi(x) > \lambda > 0$ and $\Phi = \Phi(r,\theta) \geq 0$ on $\overline{\Upsilon}$. The diffusion coefficient ε is a small positive parameter with $\Psi(r), \Phi(r,\theta)$ and $f(r,\theta)$ are sufficiently smooth function.

Now, we enforce the conditions of compatibility: $y_0(0) = 0$ and $y_0(1) = 0$; therefore, we ensure that the data aligns with the coordinates of both $(0,0)$ and $(1,0)$ in order to establish a match between the two corners. These conditions ensure the existence of a constant $\mathcal{C}$ such that, for all $(r,\theta) \in \overline{\Upsilon}_r \times \overline{\Upsilon}_\theta$ where $\overline{\Upsilon}_r = [0,1]$ and $\overline{\Upsilon}_\theta = [0,\mathfrak{T}]$ the specified inequalities hold in [4]

$$\begin{cases} |y(r,\theta) - y_0(r)| \leq \mathcal{C}\theta, \\ |y(r,\theta) - y_0(r)| \leq \mathcal{C}(1-r). \end{cases} \tag{2.2}$$

The problem reduced in the form when we putting $\varepsilon = 0$ in the problem (2.1) and observation the boundary layer at $r = 1$ is given by

$$\begin{cases} y^0_\theta + \Psi(r)y^0_r + \Phi(r,\theta)y^0 = f(r,\theta), \quad (r,\theta) \in \Upsilon_r \times \Upsilon_\theta, \\ y^0(r,0) = y_0(r), \quad 0 \leq r \leq 1, \\ y^0(0,\theta) = 0, \quad 0 < \theta \leq \mathfrak{T}. \end{cases} \tag{2.3}$$

In Equation (2.3), we observed a hyperbolic equation of first order with an initial condition mentioned along both sides $\theta = 0$ and $r = 0$ of $\overline{\Upsilon}$, where $\overline{\Upsilon} = [0,1]$. When epsilon takes on small values, the solution $y(r,\theta)$ for Equation (2.1) closely approximates $y^0(r,\theta)$. It is expected that the solution to the reduced problem (2.3) exhibits adequate smoothness in order to determine error boundaries for the solution of the above scheme.

As we now consider bounds on the derivatives of the solution $y(r,\theta)$ for Equation (2.1), it is acceptable to assume that the initial condition is zero without losing generality, as shown in references [4].

Lemma 2.1. *There exist a non-negative constant $\mathcal{C}$ such that*

$$|y(r,\theta)| \leq \mathcal{C}, \quad (r,\theta) \in \overline{\Upsilon}_r \times \overline{\Upsilon}_\theta, \quad \textit{where} \quad \overline{\Upsilon}_r = [0,1], \quad \textit{and} \quad \overline{\Upsilon}_\theta = [0,\mathfrak{T}]. \tag{2.4}$$

Proof. From the inequality $|y(r,\theta) - y(r,0)| - |y(r,\theta) - y_0(r)| \leq \mathcal{C}\theta$, we have $|y(r,\theta)| - |y_0(r)| \leq |y(r,\theta) - y_0(r,0)| \leq \mathcal{C}\theta$. That is we have, $|y(r,\theta)| \leq \mathcal{C}\theta + |y_0(r)|$. Since $\theta \in [0,\mathfrak{T}]$ and $y_0(r)$ is bounded, implies that $|y(r,\theta)| \leq \mathcal{C}$. □

3. Time discretization

Using the backward Euler approach, the continuous problem (2.1) is discretized in the temporal direction such that

$$\begin{cases} \dfrac{y_{k+1} - y_k}{\Delta\theta} - \varepsilon(y_{k+1})_{rr}(r) + \Psi(r)(y_{k+1})_r(r) + \Phi(r,\theta_{k+1})(y_{k+1})(r) = f(r,\theta_{k+1}), \quad 0 < r < 1, \quad \theta_{k+1} > 0, \\ y_0 = y_0(r), \quad 0 \leq r \leq 1, \\ y_{k+1}(0) = 0 \quad \text{and} \quad y_{k+1}(1) = 0, \end{cases} \tag{3.1}$$

where the term y_{k+1} is the solution of Equation (3.1) at the step $(k+1)^{th}$ time level. and also computed result is y_k, at the step k^{th} time level, where $\Delta\theta$ is the time step in temporary direction. The step k^{th} time level as follow $\theta_k = k\Delta\theta$.

Now,solving the Equation (3.1) and rewrite in the form as

$$\begin{cases} -\varepsilon(y_{k+1})_{rr}(r) + \Psi(r)(y_{k+1})_r(r) + (\dfrac{1}{\Delta\theta} + \Phi(r,\theta_{k+1}))(y_{k+1})(r) = \overline{f}(r,\theta_{k+1}), \\ \overline{f}(r,\theta_{k+1}) = f(r,\theta_{k+1}) + \dfrac{y_k}{\Delta\theta}, \quad 0 < r < 1, \quad \theta_{k+1} > 0, \\ y_0 = y_0(r), \quad 0 \leq r \leq 1, \\ y_{k+1}(0) = 0 \quad \text{and} \quad y_{k+1}(1) = 0, \end{cases} \tag{3.2}$$

The Equation (3.2) is also written in the operator term with the initial and boundary conditions we obtain as

$$\begin{cases} \mathfrak{L}_\varepsilon(y_{k+1}(r)) = \overline{f}(r,\theta_{k+1}), \quad 0 \le r \le 1, \\ y_0 = y_0(r), \quad 0 \le r \le 1, \\ y_{k+1}(0) = 0 \quad \text{and} \quad y_{k+1}(1) = 0, \quad \theta \ge 0, \end{cases} \tag{3.3}$$

where

$$\mathfrak{L}_\varepsilon(y_{k+1}(r)) \equiv -\varepsilon(y_{k+1})_{rr}(r) + \Psi(r)(y_{k+1})_r(r) + (\frac{1}{\Delta\theta} + \Phi(r,\theta_{k+1}))(y_{k+1})(r).$$

Lemma 3.1. (Maximum principle) *Assume that* $\vartheta_{k+1}(r) \in \mathcal{C}^2(\overline{\Upsilon}_r)$, *if* $\vartheta_{k+1}(0) \ge 0, \vartheta_{k+1}(1) \ge 0$ *and* $\mathfrak{L}_\varepsilon\vartheta_{k+1}(r) \ge 0$ *for all* $r \in \Upsilon_r$, *then* $\vartheta_{k+1}(r) \ge 0$ *for all* $r \in \overline{\Upsilon}_r$.

Proof. We suppose that there exist a $r^+ \in \overline{\Upsilon}_r$ such that $\vartheta_{k+1}(r^+) = \min_{r^+ \in \overline{\Upsilon}_r} \vartheta_{k+1}(r) < 0$, since $r^+ \in \Upsilon_r$. we apply the differential operator $\mathfrak{L}_\varepsilon$ on the ϑ at the spatial step point r^+ then we get in the form as

$$\mathfrak{L}_\varepsilon(y_{k+1}(r^+)) \equiv -\varepsilon(y_{k+1})_{rr}(r^+) + \Psi(r^+)(y_{k+1})_r(r^+) + (\frac{1}{\Delta\theta} + \Phi(r^+,\theta_{k+1}))(y_{k+1})(r^+). \tag{3.4}$$

Therefore, if we have the inequality of the mesh function $(y_{k+1})_{rr}(r^+) \ge 0$ and $(y_{k+1})_r(r^+) = 0$, then apply the Equation (3.4) and we get $\mathfrak{L}_\varepsilon\vartheta_{k+1}(r) < 0$, which is the contradiction as, $\mathfrak{L}_\varepsilon\vartheta_{k+1}(r) \ge 0$ for all $r \in \Upsilon_r$, Hence, we observed that the minimum of $\vartheta_{k+1}(r)$ is non-negative. □

Now, we defined the local truncation error of the temporal semi-discretization direction scheme of Equation (3.2). The error is $e_{k+1} \equiv y(\theta_{k+1}) - \hat{y}_{k+1}$, where $\hat{y}_{k+1}$ is the approximate solution of the boundary value problem, and following Equation (3.2) we have

$$\begin{cases} -\varepsilon(\hat{y}_{k+1})_{rr}(r) + \Psi(r)(\hat{y}_{k+1})_r(r) + (\frac{1}{\Delta\theta} + \Phi(r,\theta_{k+1}))(\hat{y}_{k+1})(r) = \overline{f}(r,\theta_{k+1}), \\ \overline{f}(r,\theta_{k+1}) = f(r,\theta_{k+1}) + \dfrac{\hat{y}_k}{\Delta\theta}, \quad 0 < r < 1, \quad \theta_{k+1} > 0, \\ \hat{y}_{k+1}(0) = 0, \quad \text{and} \quad \hat{y}_{k+1}(1) = 0. \end{cases} \tag{3.5}$$

The global error in temporal discretization, as defined at time step θ_k, arises from the local error estimates of each individual time step. This global error is expressed as $\mathbb{E} = y(r,\theta) - \hat{y}(r)$, where $y(r,\theta)$ represents the true value and $\hat{y}(r)$ denotes the computed value at the specified spatial and temporal coordinates.

Lemma 3.2. (Local error estimates) *If a positive constant* $\mathcal{C}$ *exists such that*

$$\left|\frac{\partial^p}{\partial\theta^p} y(r,\theta)\right| \le \mathcal{C}, \quad (r,\theta) \in \overline{\Upsilon}_r \times \overline{\Upsilon}_\theta, \quad 0 \le p \le 2,$$

then the local error estimates along time direction is given by

$$\| e_{k+1} \|_\infty \le \mathcal{C}(\Delta\theta)^2. \tag{3.6}$$

Proof. Since the function $\hat{y}^{k+1}$ satisfies

$$(1 + \Delta\theta\mathfrak{L}_\varepsilon)\hat{y}^{k+1}(r) - \Delta\theta f(r,\theta_{k+1}) = y(r,\theta_k),$$

and as the solution of (2.1) is smooth enough, it holds

$$\begin{aligned} y(\theta_k) &= y(\theta_{k+1}) + \Delta\theta\mathfrak{L}_\varepsilon y(\theta_{k+1}) - \Delta\theta f(\theta_{k+1}) + \int_{\theta_k}^{\theta_{k+1}} (\theta_k - z)\frac{\partial^2 y}{\partial\theta^2}(z)dz \\ &= (1 + \Delta\theta\mathfrak{L}_\varepsilon)y(\theta_{k+1}) - \Delta\theta f(\theta_{k+1}) + O(\Delta\theta^2). \end{aligned}$$

Then, the local error satisfy the following boundary value problem

$$\begin{cases} (1 + \Delta\theta\mathfrak{L}_\varepsilon)e_{k+1} = O(\Delta\theta^2), \\ e_{k+1}(0) = e_{k+1}(1) = 0. \end{cases} \tag{3.7}$$

An application of Lemma 3.1 on the operator $(1+\Delta\theta\mathfrak{L}_\varepsilon)$ gives $\| e_{k+1} \|_\infty \leq \mathcal{C}(\Delta\theta)^2$, which completes the proof. ☐

Theorem 3.3. (Global error estimates) *If a positive constant $\mathcal{C}$ exists such that*

$$\| \mathbb{E}_k \|_\infty \leq \mathcal{C}\Delta\theta, \quad \textit{for all} \quad k \leq \frac{\mathfrak{T}}{\Delta\theta}. \tag{3.8}$$

Proof. We utilizing the local error estimates up to the k^{th} time step as provided by Lemma 3.2, we can derive the subsequent global error estimate at the $(k+1)^{th}$ time step. This theorem proof detailed in [13] ☐

4. Bounds on semi-discrete problems

For the finite difference scheme, we computed the local error bound and also obtained the error bound on the exact solutions of the problem (3.1).

Theorem 4.1. *$y_{k+1}(r)$ is the exact solution of Equation (3.1) satisfies the bound as*

$$\left|\frac{d^p y_{k+1}(r)}{dr^p}\right| \leq \mathcal{C}(1+\varepsilon^{-p}exp(-\lambda(1-r)/\varepsilon)), \quad 0 \leq p \leq 4. \tag{4.1}$$

Proof. The maximum principle applied to the function $\mathfrak{L}_\varepsilon$, along with the stipulated smoothness conditions for both f and y, leads to the conclusion that the absolute value of $\| y_{k+1} \| \leq (C)$ is bounded. The demonstration of the bounds for its derivatives can be obtained through a similar approach as outlined in reference [18]. ☐

4.1. **Decomposition of the Solution.** Given that the existing constraints on the solution's derivatives are insufficiently precise for establishing $\varepsilon-$uniform convergence, it becomes necessary to establish more robust bounds. These enhanced bounds are derived through a method initially proposed by Shishkin, involving the decomposition of the solution into its smooth and singular components. Suppose that the solution $y_{k+1}(r)$ at the time level $(k+1)^{th}$ is divided into two part: a smooth component $\mathcal{A}_{k+1}(r)$ and a singular component $\mathcal{B}_{k+1}(r)$ at the $(k+1)^{th}$ time level. We defined in the term and follows that

$$y_{k+1}(r) = \mathcal{A}_{k+1}(r) + \mathcal{B}_{k+1}(r), \quad \text{for} \quad 0 \leq r \leq 1,$$

since the smooth component adheres to the non-homogeneous problem and singular component homogeneous, where its characteristics fulfil the specified conditions

$$\begin{cases} -\varepsilon(\mathcal{A}_{k+1})_{rr}(r) + \Psi(r)(\mathcal{A}_{k+1})_r(r) + (\dfrac{1}{\Delta\theta} + \Phi(r,\theta_{k+1}))(\mathcal{A}_{k+1})(r) = \overline{f}(r,\theta_{k+1}), \\ \overline{f}(r,\theta_{k+1}) = f(r,\theta_{k+1}) + \dfrac{\mathcal{A}_k}{\Delta\theta}, \quad 0 \leq r \leq 1, \\ \mathcal{A}_{k+1}(1) = ((\mathcal{A}_{k+1})_0 + \varepsilon(\mathcal{A}_{k+1})_1)(1), \\ \mathcal{A}_{k+1}(0) = y_{k+1}(0), \end{cases} \tag{4.2}$$

here the singular component adheres to the homogeneous problem and we drive in the form as

$$\begin{cases} -\varepsilon(\mathcal{B}_{k+1})_{rr}(r) + \Psi(r)(\mathcal{B}_{k+1})_r(r) + (\dfrac{1}{\Delta\theta} + \Phi(r,\theta_{k+1}))(\mathcal{B}_{k+1})(r) = 0, \quad 0 \leq r \leq 1, \\ \mathcal{B}_{k+1}(1) = y_{k+1}(1) - \mathcal{B}_{k+1}(1), \\ \mathcal{B}_{k+1}(0) = 0. \end{cases} \tag{4.3}$$

Now, We proceed with additional decomposition within the smooth component, denoted as $\mathcal{A}$.

$$\mathcal{A}_{k+1}(r) = ((\mathcal{B}_{k+1})_0 + \varepsilon(\mathcal{A}_{k+1})_1 + \varepsilon^2(\mathcal{A}_{k+1})_2)(r), \quad 0 \leq r \leq 1,$$

where $(\mathcal{A}_{k+1})_0$ is the solution of reduced problem

$$\begin{cases} \Psi(r)((\mathcal{A}_{k+1})_1)_r + (\dfrac{1}{\Delta\theta} + \Phi(r,\theta_{k+1}))(\mathcal{A}_{k+1})_1 = ((\mathcal{A}_{k+1})_0)_{rr}, \quad 0 \leq r \leq 1, \\ (\mathcal{A}_{k+1})_1(0) = 0, \end{cases} \tag{4.4}$$

$$\begin{cases} -\varepsilon((\mathcal{A}_{k+1})_2)_{rr}(r) + \Psi(r)((\mathcal{A}_{k+1})_2)_r(r) + (\dfrac{1}{\Delta\theta} + \Phi(r,\theta_{k+1}))(\mathcal{A}_{k+1})_2(r) = 0, \quad 0 \le r \le 1, \\ (\mathcal{A}_{k+1})_2(0) = (\mathcal{A}_{k+1})_1(1) = 0, \end{cases} \tag{4.5}$$

where $(\mathcal{A}_{k+1})_1$ and $(\mathcal{A}_{k+1})_2$ is the solution of the Equations (4.4) and (4.5) respectively.

Presently, we derive the bounds and derivatives for both the smooth component $\mathcal{A}_{k+1}$ and the singular component $\mathcal{B}_{k+1}$. The subsequent theorem is established for the smooth component $\mathcal{A}_{k+1}$ and the singular component $\mathcal{B}_{k+1}$ as outlined below.

Theorem 4.2. *Suppose the the solution $\mathcal{A}_{k+1}$ of the Equation (4.2) , $\mathcal{A}_{k+1}$ and their derivatives hold for the bounds*

$$\| \mathcal{A}^s_{k+1} \| \le \mathcal{C}(1+\varepsilon^{2-s}), \quad s = 0,1,2. \tag{4.6}$$

and in general term the bounds on the derivatives of $\mathcal{A}_{k+1}$ and satisfy we get as

$$\| \mathcal{A}^s_{k+1} \| \le \mathcal{C}, \quad s = 0,1,2,3. \tag{4.7}$$

Proof. Given that $(\mathcal{A}_{k+1})_0$ and $(\mathcal{A}_{k+1})_1$ represent the solutions to Equations (2.3) and (4.4), then it follows that the bounds for the solution $(\mathcal{A}_{k+1})_0$ and $(\mathcal{A}_{k+1})_1$ and also we apply the Theorem 3.3 for the solution $(\mathcal{A}_{k+1})_2$, where $(\mathcal{A}_{k+1})_2$ is the solution of the Equation (4.5) and we get the inequality of the bounds as below

$$\| (\mathcal{A}^s_{k+1})_0 \| \le \mathcal{C}, \quad \text{for} \quad 0 \le s \le 3, \tag{4.8}$$

$$\| (\mathcal{A}^s_{k+1})_1 \| \le \mathcal{C}, \quad \text{for} \quad 0 \le s \le 3, \tag{4.9}$$

$$\| (\mathcal{A}^s_{k+1})_2 \| \le \mathcal{C} + \mathcal{C}\varepsilon^{-s}e^{-\lambda(1-r)/\varepsilon}, \quad \text{for} \quad 0 \le s \le 3, \tag{4.10}$$

therefore, combining all three equation of estimates and we obtain the inequality in the form as

$$\begin{aligned} \| \mathcal{A}^s_{k+1} \| &\le \| (\mathcal{A}^s_{k+1})_0 \| + \| (\mathcal{A}^s_{k+1})_1 \| + \| (\mathcal{A}^s_{k+1})_2 \| \\ &\le \mathcal{C} + \varepsilon\mathcal{C} + \varepsilon^2(\mathcal{C} + \mathcal{C}\varepsilon^{-s}e^{-\lambda(1-r)/\varepsilon}) \\ &\le \mathcal{C} + \mathcal{C}\varepsilon^{2-s}e^{-\lambda(1-r)/\varepsilon} \\ &\le \mathcal{C}(1+\varepsilon^{2-s}), \quad \text{since} \quad e^{-\lambda(1-r)/\varepsilon} \le 1, \ \mathcal{C}, \quad \text{for} \quad s = 0,1,2, \end{aligned}$$

and also hold for $s = 3$, see in [23]. This completes the proof. □

Now, we have driven the bounds on the singular component $\mathcal{B}_{k+1}$, which satisfy the homogeneous problem of Equation (4.3) , and the theorem follows as follows:

Theorem 4.3. *Suppose that the solution $\mathcal{B}_{k+1}(r)$ of the singular component which defined in Equation (4.3), the bounds of $\mathcal{B}_{k+1}$ and its derivative verify the following estimate*

$$\| \mathcal{B}^s_{k+1}(r) \| \le \mathcal{C}\varepsilon^{-s}e^{-\lambda(1-r)/\varepsilon}, \quad \textit{for} \quad 0 \le s \le 3, \quad \textit{and} \quad 0 \le r \le 1. \tag{4.11}$$

Proof. We will be prove the theorem for $s = 0,1,2,3$. Initially, we establish the result for $s = 0$. Delve into the consideration of barrier functions

$$\vartheta^{\pm}_{k+1}(r) = \mathcal{C}e^{-\lambda(1-r)/\varepsilon} \pm \mathcal{B}^s_{k+1}(r), \quad 0 \le r \le 1. \tag{4.12}$$

Now, we find the values of the $\mathcal{B}^s_{k+1}(r)$ at the boundary point 0 and 1 such that

$$\vartheta^{\pm}_{k+1}(0) = \mathcal{C}e^{-\lambda(1-0)/\varepsilon} \pm \mathcal{B}^s_{k+1}(0),$$
$$\vartheta^{\pm}_{k+1}(0) = \mathcal{C}e^{-\lambda/\varepsilon} \ge 0,$$

and boundary point at 1 we have

$$\begin{aligned} \vartheta^{\pm}_{k+1}(1) &= \mathcal{C}e^{-\lambda(1-1)/\varepsilon} \pm \mathcal{B}^s_{k+1}(1), \\ &= \mathcal{C}e^{0} \pm \mathcal{B}^s_{k+1}(1), \end{aligned}$$

hence,

$$\vartheta^{\pm}_{k+1}(1) = \mathcal{C} \pm \mathcal{B}^s_{k+1}(1) \ge 0.$$

Hence, we employ the Lemma 3.1 of the maximum principle on the derivative operator $\mathfrak{L}_\varepsilon$, leading to the obtained result

$$\mathfrak{L}_\varepsilon \vartheta^{\pm}_{k+1}(r) = (-\varepsilon(\vartheta^{\pm}_{k+1})_{rr} + \Psi(r)(\vartheta^{\pm}_{k+1})_r + (\frac{1}{\Delta\theta} + \Phi(r,\theta_{k+1})\vartheta^{\pm}_{k+1}(r), \quad \text{for all} \quad r \in \overline{\Upsilon}_r, \tag{4.13}$$

differentiate with respect to r of barrier functions $\vartheta^{\pm}_{k+1}(r)$ which defined in the Equation (4.12) and put all result in the Equation (4.13) we get

$$\begin{aligned}(-\varepsilon(\vartheta^{\pm}_{k+1})_{rr} &+ \Psi(r)(\vartheta^{\pm}_{k+1})_r + (\frac{1}{\Delta\theta} + \Phi(r,\theta_{k+1})\vartheta^{\pm}_{k+1}(r)\\
&\geq \mathcal{C}e^{-\lambda(1-r)/\varepsilon}\Big[-\frac{\lambda^2}{\varepsilon} + \Psi(r)\frac{\lambda}{\varepsilon} + (\frac{1}{\Delta\theta} + \Phi(r,\theta_{k+1}) + 1\Big], \quad \text{for all} \quad r \in \overline{\Upsilon}_r,\\
&\geq \mathcal{C}e^{-\lambda(1-r)/\varepsilon} \geq 0, \quad \text{for all} \quad r \in \overline{\Upsilon}_r,\end{aligned}$$

hence,

$$\| \mathcal{B}^s_{k+1}(r) \| \leq \mathcal{C}\varepsilon^{-s}e^{-\lambda(1-r)/\varepsilon}, \quad \text{for} \quad 0 \leq s \leq 3, \quad \text{and} \quad 0 \leq r \leq 1,$$

and also true for $s = 1,2,3$ see in [7]. This completes the proof. □

5. Spatial discretization

In this section, to construct the numerical method, we utilized a non-uniform mesh, defined as classical Shishkin meshes, Shishkin-Bakhvalov meshes, and Shishkin-Bakhvalov modified meshes, which are determined by the generating function with the boundary layer at the right side of the domain. We also described the midpoint finite difference scheme and applied it to the above meshes.

First, we divided the interval $[0,1]$ into two parts: $\big[0,1-\gamma\big]$ and $\big[1-\gamma,1\big]$, where γ is the transition parameter that depends on ε and $\mathcal{N}$, since ε is the perturbation parameter and $\mathcal{N}$ represents the number of grid points in space. The transition parameter $\gamma = \min\{1/2, \kappa\varepsilon\ln\mathcal{N}\}$, where κ is a non-negative constant that will be fixed later. If the parameter γ is set to $1/2$, the mesh will exhibit uniformity, enabling a classical analysis approach. Throughout the rest of the paper, we assume that γ is equal to $\kappa\varepsilon\ln\mathcal{N}$, representing the most practically significant scenario. Within the interval $\big[0,1-\gamma\big]$, we employ a uniform mesh with designated points $r_0 = 0$ and $r_{\mathcal{N}/2} = 1-\gamma$. However, for the interval $\big[1-\gamma,1\big]$, the mesh adopts a graded structure, ensuring that the step sizes, denoted as $h_k = r_k - r_{k-1}$, adhere to the condition $h_k \geq h_k + 1$ for $k = \mathcal{N}/2+1,...,\mathcal{N}-1$. We define the mesh by employing a continuous, monotonically increasing, and piecewise continuously differentiable function $\varphi(s^*)$. Since $s^* \in \big[1/2,1\big]$ such that $\varphi(1/2) = -\ln\mathcal{N}$ and $\varphi(1/2) = 0$. then, the mesh points are given by

$$r_k = \begin{cases} 2(1-\gamma)k/\mathcal{N}, & k = 0,...,\mathcal{N}/2,\\ 1+\kappa\varepsilon\varphi(s^*_k), \quad s^*_k = k/\mathcal{N}, & k = \mathcal{N}/2+1,...,\mathcal{N}.\end{cases} \tag{5.1}$$

Therefore, according to the mesh explanation we have

$$h_k = \mathcal{H} = 2(1-\gamma)/\mathcal{N}, \quad k = 1,2,3,...,\mathcal{N}/2 \quad \text{and} \quad \mathcal{N}^{-1} \leq \mathcal{H} \leq 2\mathcal{N}^{-1}.$$

Again, suppose that new function $g(s^*) = \exp(\varphi(s^*))$ and also increasing and verify $g(1/2) = \mathcal{N}^{-1}$ and $g(1) = 1$. The three different meshes function define as following

- **Shishkin mesh**

$$g(s^*) = e^{-(2-2s^*)2\ln\mathcal{N}}. \tag{5.2}$$

- **Shishkin-Bakhvalov mesh**

$$g(s^*) = 1-(2-2\mathcal{N}^{-1})(2-2s^*). \tag{5.3}$$

- **Shishkin-Bakhvalov modified mesh**

$$g(s^*) = e^{-(1-s^*)/((\dfrac{1}{2}+\dfrac{1}{2\ln\mathcal{N}})-(1-s^*))}. \tag{5.4}$$

Now, we initiate the presentation of certain properties associated with these meshes, which will be essential for subsequent discussions.

Lemma 5.1. *The mesh defined in Equation (5.1) for $k = \mathcal{N}/2+1,...,\mathcal{N}$, satisfies the following inequality*

$$h_k \le \kappa\varepsilon\mathcal{N}^{-1} \max_{s^*\in[1/2,1]} \left|\varphi'(s^*)\right|, \tag{5.5}$$

$$(h_k/\varepsilon)^\lambda e^{-\lambda(1-r_k)/\kappa\varepsilon} \le \mathcal{C}\left(\kappa\mathcal{N}^{-1} \max_{s^*\in[1/2,1]} \left|g'(s^*)\right|\right)^\lambda, \tag{5.6}$$

Again, the mesh defined by (5.2) and satisfy the bound

$$h_k = 2\kappa\varepsilon\mathcal{N}^{-1}\ln\mathcal{N}, \tag{5.7}$$

For mesh defined in Equation (5.3),

$$h_k \le 2\kappa\varepsilon/(k-\mathcal{N}/2), \quad \textit{for} \quad k = \mathcal{N}/2+1,...,\mathcal{N}, \tag{5.8}$$

and the mesh given by (5.4) for $k = \mathcal{N}/2+1,...,\mathcal{N}$,

$$h_k \le \mathcal{C}_2\varepsilon\mathcal{N}^{-1}\ln^2\mathcal{N}, \quad h_\mathcal{N} \le \mathcal{C}_3\varepsilon\mathcal{N}^{-1}. \tag{5.9}$$

Proof. The bounds of mesh which is defined in Equations (5.5) and (5.6) brief proof in [8] for $\lambda = 1$ and also holds for $\lambda \ge 2$. The bound in Equation (5.8) proof in [16] and also easily proof by definition of mesh for the bound in Equation (5.9). □

5.1. **finite difference scheme.** Before, we defined some useful finite difference operators of first order and second order, which are used in the proposed method.

$$\begin{cases} D_r^+ z(r_i,\theta_n) = \dfrac{z(r_{i+1},\theta_n) - z(r_i,\theta_n)}{h_{i+1}}, \\ D_r^- z(r_i,\theta_n) = \dfrac{z(r_i,\theta_n) - z(r_{i-1},\theta_n)}{h_i}, \\ D_r^0 z(r_i,\theta_n) = \dfrac{z(r_{i+1},\theta_n) - z(r_{i-1},\theta_n)}{\hat{h_i}}, \\ D_\theta^- z(r_i,\theta_n) = \dfrac{z(r_i,\theta_n) - z(r_i,\theta_{n-1})}{\triangle\theta}, \end{cases} \tag{5.10}$$

respectively, and define the second order finite difference operator δ_r^2 in space by

$$\delta_r^2 z(r_i,\theta_n) = \frac{2\left(D_r^+ z(r_i,\theta_n) - D_r^- z(r_i,\theta_n)\right)}{\hat{h_i}},$$

where $\hat{h_i} = h_j + h_{i+1}$ $i = 1,...,N-1$ and $h_i = r_i - r_{i-1}$, $i = 1,...N$.

Now, we apply the midpoint finite difference scheme on the classical Shishkin meshes, Shishkin-Bakhvalov meshes, and Shishkin-Bakhvalov modified meshes.

$$\begin{cases} \dfrac{Y_{k+1}^\mathcal{N}(r_i) - Y_k^\mathcal{N}(r_i)}{\Delta\theta} - \varepsilon\delta^2 Y_{k+1}^\mathcal{N}(r_i) + \Psi(r_{i-1/2})\mathcal{D}^- Y_{k+1}^\mathcal{N}(r_i) + \Phi(x_{i-1/2},\theta_{k+1})Y_{k+1}^\mathcal{N}(r_i) = f(r_{i-1/2},\theta_{k+1}), \\ Y_0^\mathcal{N}(r_i) = y_0(r_i), \quad r_i \in \Upsilon_r^\mathcal{N}, \\ Y_{k+1}^\mathcal{N}(r_0) = 0, \quad \text{and} \quad Y_{k+1}^\mathcal{N}(r_\mathcal{N}) = 0, \end{cases} \tag{5.11}$$

where the approximate solution $Y_{K+1}^\mathcal{N}(r_i)$ of $y_{K+1}(r_i)$ at the points $r_i, i = 0,1,2,...,\mathcal{N}$.

Now, we applied the operator $\mathfrak{L}_\varepsilon^\mathcal{N}$ on the Equation (5.11) and we have new equation in the operator form as

$$\begin{cases} \mathfrak{L}_\varepsilon^\mathcal{N} Y_{k+1}^\mathcal{N}(r_i) = f(r_{i-1/2,\theta_{k+1}}) + \dfrac{Y_k^{\mathcal{N}(r_i)}}{\Delta\theta}, \quad r_i \in \Upsilon_r^\mathcal{N}, \\ Y_0^\mathcal{N}(r_i) = y_0(r_i), \quad r_i \in \Upsilon_r^\mathcal{N}, \\ Y_{k+1}^\mathcal{N}(0) = 0, \quad \text{and} \quad Y_{k+1}^\mathcal{N}(1) = 0, \end{cases} \tag{5.12}$$

where the operator $\mathfrak{L}_\varepsilon^{\mathcal{N}}$ is given by

$$\mathfrak{L}_\varepsilon^{\mathcal{N}} \equiv -\varepsilon\delta^2 + \Psi(r_{i-1/2})\mathcal{D}^- + (\Phi(r_{1-1/2}, \theta_{k+1}) + \frac{1}{\Delta\theta})I, \tag{5.13}$$
$$\Psi(r_{i-1/2}) = \frac{\Psi(r_{i-1}) + \Psi(r_i)}{2}, \quad \text{and} \quad \Phi(r_{i-1/2}, \theta_{k+1}) = \frac{\Psi(r_{i-1}, \theta_{k+1}) + \Psi(r_i), \theta_{k+1}}{2},$$
$$f_{k+1}(r_{i-1/2}) = \frac{f_{k+1(r_{i-1})+f_{k+1}(r_i)}}{2}.$$

6. Stability and convergence analysis

Lemma 6.1. (Discrete Maximum Principle) *The discrete operator $\mathfrak{L}_\varepsilon^{\mathcal{N}}$ satisfies a discrete maximum principle, i.e. if $\{\Theta_i\}$ and $\{\vartheta_i\}$ are the mesh function satisfies $\Theta_0 \le \vartheta_0$ and $\mathfrak{L}_\varepsilon^{\mathcal{N}}\Theta_i \le \mathfrak{L}_\varepsilon^{\mathcal{N}}\vartheta_i$ for $i = 1, 2, ..., \mathcal{N}-1$, then $\Theta_i \le \vartheta_i$ for all i.*

Proof. The matrix linked with $\mathfrak{L}_\varepsilon^{\mathcal{N}}$ has dimensions $(\mathcal{N}+1) \times (\mathcal{N}+1)$ and fulfills the criteria of being an $\mathcal{M}$-matrix. Consequently, it is classified as an $\mathcal{M}$-matrix. □

Lemma 6.2. *Suppose that $\mathcal{Q}_{k+1} = 1 + r_i$ for $0 \le i \le \mathcal{N}$. then there exist a non-negative constant $\mathcal{C}$ such that $\mathfrak{L}_\varepsilon^{\mathcal{N}}\mathcal{Q}_{k+1}(r_i) \ge \mathcal{C}$ for $1 \le i \le \mathcal{N}-1$.*

Proof. This proof is very easy calculation. □

Lemma 6.3. *The mesh function is defined for a fixed value of k, with i ranging from 0 to $\mathcal{N}$ such that*

$$\mathcal{G}_{k+1}(r_i) = \prod_{p=1}^{i}\left(1 + \frac{\lambda h_p}{\varepsilon}\right),$$

with usual convention that if $i = 0$, then $\mathcal{G}_0 = 1$. then for $i = 1, 2, ..., \mathcal{N}-1$, we have

$$\mathfrak{L}_\varepsilon^{\mathcal{N}}\mathcal{G}_{k+1}(r_i) \ge \frac{\mathcal{C}}{max\{\varepsilon, h_i\}}\mathcal{G}_{k+1}(r_i),$$

for some constant $\mathcal{C}$.

Proof. Now, we can write the inequality in the form as

$$\begin{aligned}
\frac{\mathcal{G}_{k+1}(r_i) - \mathcal{G}_{k+1}(r_{i-1})}{h_i} &= \frac{\lambda\mathcal{G}_{k+1}(r_{i-1})}{\varepsilon}, \\
\mathfrak{L}_\varepsilon^{\mathcal{N}}\mathcal{G}_{k+1}(r_i) &= \frac{-2\varepsilon}{h_i + h_{i+1}}\frac{\lambda(\mathcal{G}_{k+1}(r_i) - \mathcal{G}_{k+1}(r_{i-1}))}{\varepsilon} \\
&+ \Psi_{i-1/2}\frac{\lambda\mathcal{G}_{k+1}(r_{i-1})}{\varepsilon} + (\Phi(r_{1-1/2}, \theta_{k+1}) + \frac{1}{\Delta\theta})\mathcal{G}_{k+1}(r_i), \\
&= \frac{\lambda}{\varepsilon}\mathcal{G}_{k+1}(r_{i-1})\left(\Psi_{i-1/2} - \frac{2\lambda h_i}{h_i + h_{i+1}}\right) + (\Phi(r_{1-1/2}, \theta_{k+1}) + \frac{1}{\Delta\theta})\mathcal{G}_{k+1}(r_i), \\
&= \frac{\lambda}{\varepsilon + h_i}\mathcal{G}_{k+1}(r_i)\left(\Psi_{i-1/2} - \frac{2\lambda h_i}{h_i + h_{i+1}} + (\Phi(r_{1-1/2}, \theta_{k+1}) + \frac{1}{\Delta\theta})\frac{\varepsilon + \lambda h_i}{\lambda}\right),
\end{aligned}$$

from which the result follows. □

Lemma 6.4. *Suppose that $\mathcal{V}_{k+1}(r)$ be any smooth function defined on the interval $[0, 1]$. For $i = 1, 2, ..., \mathcal{N}-1$, and define the truncation error of $\mathfrak{L}_\varepsilon^{\mathcal{N}}$ to $\mathcal{V}_{k+1}(r)$ at $r_{i-1/2}$ to be $\mathfrak{L}_\varepsilon^{\mathcal{N}}(\mathcal{V}_{k+1}(r_i)) - (\mathfrak{L}_\varepsilon\mathcal{V}_{k+1})(r_{i-1/2})$. Then there exist a constant $\mathcal{C}$ such that*

$$\left|\mathfrak{L}_\varepsilon^{\mathcal{N}}(\mathcal{V}_{k+1}(r_i)) - (\mathfrak{L}_\varepsilon\mathcal{V}_{k+1})(r_{i-1/2})\right| \le \mathcal{C}\varepsilon\int_{r_{i-1}}^{r_{i+1}}\left|\mathcal{V}_{k+1}'''(\zeta)\right|d\zeta + \mathcal{C}h_i\int_{r_{i-1}}^{r_i}\left|\mathcal{V}_{k+1}'''(\zeta)\right|d\zeta. \tag{6.1}$$

Proof. The proof is similar of this Lemma to the proof of Lemma 3.3 in [14]. □

Lemma 6.5. *For each i, we have*

$$e^{-\lambda(1-r_i)/\varepsilon} \leq \prod_{p=i+1}^{\mathcal{N}} \left(1+\frac{\lambda h_p}{\varepsilon}\right)^{-1}.$$

Proof. For each p, we have

$$e^{-\lambda h_p/\varepsilon} = (e^{-\lambda h_p/\varepsilon})^{-1} \leq \left(1+\frac{\lambda h_p}{\varepsilon}\right)^{-1}.$$

Now, multiplying these inequality for $p = i+1, 2, ..., \mathcal{N}$ and we get the desired result. □

Lemma 6.6. *For the Shishkin mesh which is defined in Equation (5.2) and there exists a constant $\mathcal{C}$ such that*

$$\prod_{p=i+1}^{\mathcal{N}} \left(1+\frac{\lambda h_p}{\varepsilon}\right)^{-1} \leq \mathcal{C}\mathcal{N}^{-4(1-i/\mathcal{N})}, \quad \mathcal{N}/2 \leq i \leq \mathcal{N}.$$

Proof. Suppose that $\mathcal{N}/2 \leq i \leq \mathcal{N}$, through the Lemma 4.1(b) which described by Kellogg and Tsan in [14]

$$\begin{aligned}
\prod_{p=i+1}^{\mathcal{N}} \left(1+\frac{\lambda h_p}{\varepsilon}\right)^{-1} &\leq e^{-\lambda(1-r_i)/(\varepsilon+\lambda h_i)}, \\
&= e^{-4(\mathcal{N}-i)(\mathcal{N}^{-1}\ln\mathcal{N})/(1+4\mathcal{N}^{-1}\ln\mathcal{N})} \\
&= \mathcal{N}^{-4(\mathcal{N}-i)\mathcal{N}^{-1}/(1+4\mathcal{N}^{-1}\ln\mathcal{N}))},
\end{aligned}$$

hence,

$$\mathcal{N}^{-4(1-i/\mathcal{N})}\mathcal{N}^{16(1-i/\mathcal{N})(\mathcal{N}^{-1}\ln\mathcal{N}/(1+4\mathcal{N}^{-1}\ln\mathcal{N})}.$$

Since $\mathcal{N}^{16(1-i/\mathcal{N})(\mathcal{N}^{-1}\ln\mathcal{N}/(1+4\mathcal{N}^{-1}\ln\mathcal{N})}$ is bounded for $\mathcal{N} \geq 2$, therefore we obtained the required result. □

6.1. **Decomposition of Numerical solution.** We break down the numerical solution $Y_{k+1}^{\mathcal{N}}$ into its smooth $\hat{\mathcal{A}}_{k+1}^{\mathcal{N}}(r_i)$ and singular $\hat{\mathcal{B}}_{k+1}^{\mathcal{N}}(r_i)$ components. This decomposition is described in the same manner as the semi-discrete process.

$$Y_{k+1}^{\mathcal{N}}(r_i) = \hat{\mathcal{A}}_{k+1}^{\mathcal{N}}(r_i) + \hat{\mathcal{B}}_{k+1}^{\mathcal{N}}(r_i),$$

now, the smooth component $\hat{\mathcal{A}}_{k+1}^{\mathcal{N}}(r_i)$ satisfies the non-homogeneous equation

$$\begin{cases} \mathfrak{L}_{\varepsilon}^{\mathcal{N}}\hat{\mathcal{A}}_{k+1}^{\mathcal{N}}(r_i) = \overline{f}(r_{i-1/2}, \theta_{k+1}), \\ \hat{\mathcal{A}}_{k+1}^{\mathcal{N}}(0) = \mathcal{A}_{k+1}(0), \\ \hat{\mathcal{A}}_{k+1}^{\mathcal{N}}(1) = \mathcal{A}_{k+1}(1), \end{cases} \tag{6.2}$$

and the singular component $\hat{\mathcal{B}}_{k+1}^{\mathcal{N}}(r_i)$ satisfies the homogeneous equation

$$\begin{cases} \mathfrak{L}_{\varepsilon}^{\mathcal{N}}\hat{\mathcal{B}}_{k+1}^{\mathcal{N}}(r_i) = 0, \\ \hat{\mathcal{B}}_{k+1}^{\mathcal{N}}(0) = \mathcal{B}_{k+1}(0), \\ \hat{\mathcal{B}}_{k+1}^{\mathcal{N}}(1) = \mathcal{B}_{k+1}(1), \end{cases} \tag{6.3}$$

The error in the numerical solution can now be broken down into components as well.

$$\big(Y_{k+1}^{\mathcal{N}} - y_{k+1}\big)(r_i) = \big(\hat{\mathcal{A}}_{k+1}^{\mathcal{N}} - \mathcal{A}_{k+1}\big)(r_i) + \big(\hat{\mathcal{B}}_{k+1}^{\mathcal{N}} - \mathcal{B}_{k+1}\big)(r_i),$$

we separately estimate the error in both smooth and singular solutions.

Theorem 6.7. (Error in the smooth component) *The smooth component error $\hat{\mathcal{A}}_{k+1}^{\mathcal{N}}$ adheres to the subsequent estimate at the $(k+1)$th time step.*

$$\left|\mathcal{A}_{k+1}(r_i) - \hat{\mathcal{A}}_{k+1}^{\mathcal{N}}(r_i)\right| \leq \mathcal{C}\mathcal{N}^{-1}\Big(\varepsilon + \mathcal{N}^{-1}\Big), \quad r_i \in \overline{\Upsilon}_r. \tag{6.4}$$

Proof. We have proof the error in the smooth part such that

$$\left|\mathfrak{L}_{\varepsilon}^{\mathcal{N}}\left(\mathcal{A}_{k+1}(r_i)-\hat{\mathcal{A}}_{k+1}^{\mathcal{N}}(r_i)\right)\right|=\left|\left(\mathfrak{L}_{\varepsilon}^{\mathcal{N}}\mathcal{A}_{k+1}(r_i)\right)-\left(\mathfrak{L}_{\varepsilon}^{\mathcal{N}}\mathcal{A}_{k+1}(r_{i-1/2})\right)\right|\leq\mathcal{N}(\varepsilon+h_i)(h_i+h_{i+1}),$$

we utilised the Lemma 6.4. Now, we applied the barrier function $\vartheta_{k+1}(r_i)=\mathcal{C}\mathcal{H}(\varepsilon+\mathcal{H})(1+r_i)$, where $\mathcal{H}=max_i\{h_i\}$ and also applying the Lemmas 6.1 and 6.2 we get the result

$$\left|\mathcal{A}_{k+1}(r_i)-\hat{\mathcal{A}}_{k+1}^{\mathcal{N}}(r_i)\right|\leq\mathcal{C}\mathcal{H}\left(\varepsilon+\mathcal{H}\right)=\mathcal{C}\mathcal{N}^{-1}\left(\varepsilon+\mathcal{N}^{-1}\right),$$

Hence

$$\left|\mathcal{A}_{k+1}(r_i)-\hat{\mathcal{A}}_{k+1}^{\mathcal{N}}(r_i)\right|\leq\mathcal{C}\mathcal{N}^{-1}\left(\varepsilon+\mathcal{N}^{-1}\right),\quad r_i\in\overline{\Upsilon}_r.$$

□

Theorem 6.8. (Error in the singular component) *The singular component error $\hat{\mathcal{B}}_{k+1}^{\mathcal{N}}$ adheres to the subsequent estimate at the $(k+1)$th time step.*

$$\left|\mathcal{B}_{k+1}(r_i)-\hat{\mathcal{B}}_{k+1}^{\mathcal{N}}(r_i)\right|\leq\begin{cases}\mathcal{C}\mathcal{N}^{-2}, & for\quad 0\leq i<\mathcal{N}/2,\\ \mathcal{C}\mathcal{N}^{-1}\left(\varepsilon+\mathcal{N}^{-4(1-i/\mathcal{N})\ln\mathcal{N}}\right), & for\quad \mathcal{N}/2\leq i\leq\mathcal{N}.\end{cases}\tag{6.5}$$

Proof. We consider the barrier function $\vartheta_{k+1}(r_i)$ such that

$$\vartheta_{k+1}(r_i)=\mathcal{C}\left[\prod_{p=i+1}^{\mathcal{N}}\left(1+\frac{\lambda h_p}{\varepsilon}\right)^{-1}\right]\mathcal{G}_{k+1}(r_i),$$

again we utilise the Lemma 6.1 of the discrete maximum principle such that

$$\left|\hat{\mathcal{B}}_{k+1}^{\mathcal{N}}(r_i)\right|\leq\vartheta_{k+1}(r_i)=\mathcal{C}\left[\prod_{p=i+1}^{\mathcal{N}}\left(1+\frac{\lambda h_p}{\varepsilon}\right)^{-1}\right]\mathcal{G}_{k+1}(r_i).\tag{6.6}$$

Now, we calculate the estimate $\left|\mathcal{B}_{k+1}(r_i)-\hat{\mathcal{B}}_{k+1}^{\mathcal{N}}(r_i)\right|$, using Equations (4.11) and (6.6) also apply the Lemma 6.5 obtained the result

$$\left|\mathcal{B}_{k+1}(r_i)-\hat{\mathcal{B}}_{k+1}^{\mathcal{N}}(r_i)\right|\leq\mathcal{C}\prod_{p=i+1}^{\mathcal{N}}\left(1+\frac{\lambda h_p}{\varepsilon}\right)^{-1}.$$

Once more, we establish the inequality defined in Equation (6.5) for $0\leq i<\mathcal{N}/2$ and $\mathcal{N}/2\leq i\leq\mathcal{N}$ as follows: for $0\leq i<\mathcal{N}/2$, we used the Lemma 6.6 in the above inequality result and taking $i=\mathcal{N}/2$

$$\left|\mathcal{B}_{k+1}(r_{\mathcal{N}/2})-\hat{\mathcal{B}}_{k+1}^{\mathcal{N}}(r_{\mathcal{N}/2})\right|\leq\mathcal{C}\mathcal{N}^{-2}.\tag{6.7}$$

Furthermore, $\left|\mathcal{B}_{k+1}(r_{\mathcal{N}/2})-\hat{\mathcal{B}}_{k+1}^{\mathcal{N}}(r_{\mathcal{N}/2})\right|=0$.

Now, we rewrite the Lemma 6.4 for the range $\mathcal{N}/2<i<\mathcal{N}$ such that

$$\left|\mathfrak{L}_{\varepsilon}^{\mathcal{N}}(\mathcal{V}_{k+1}(r_i))-(\mathfrak{L}_{\varepsilon}\mathcal{V}_{k+1})(r_{i-1/2})\right|\leq\mathcal{C}\int_{r_{i-1}}^{r_{i+1}}\left[\varepsilon\left|\mathcal{V}_{k+1}^{'''}(\zeta)\right|+\left|\mathcal{V}_{k+1}^{''}(\zeta)\right|\right]d\zeta.\tag{6.8}$$

For the range $\mathcal{N}/2<i<\mathcal{N}$, we calculated the error estimate of the singular component by using Equation (6.8) and the Lemma 6.5 obtained the result.

$$\left|\mathfrak{L}_{\varepsilon}^{\mathcal{N}}\left(\mathcal{B}_{k+1}(r_i)-\hat{\mathcal{B}}_{k+1}^{\mathcal{N}}(r_i)\right)\right|\leq\left(\mathcal{C}\varepsilon^{-1}\mathcal{N}^{-1}\ln\mathcal{N}\right)\prod_{p=i+1}^{\mathcal{N}}\left(1+\frac{\lambda h_p}{\varepsilon}\right)^{-1},$$

Now, we build the barrier function $\vartheta_{k+1}(r_i)$ such that

$$\vartheta_{k+1}(r_i) \leq \mathcal{C}\Big(\mathcal{N}^{-2} + (\mathcal{N}^{-1}\ln\mathcal{N})\Big[\prod_{p=i+1}^{\mathcal{N}}\Big(1+\frac{\lambda h_p}{\varepsilon}\Big)^{-1}\Big]\mathcal{G}_{k+1}(r_i)\Big).$$

Again, we proof for the range $\mathcal{N}/2 \leq i \leq \mathcal{N}$, and apply the Lemma 6.1 also utilised the barrier function $\vartheta_{k+1}(r_i)$ which is the above defined and obtained the result

$$\Big|\mathcal{B}_{k+1}(r_i) - \hat{\mathcal{B}}^{\mathcal{N}}_{k+1}(r_i)\Big| \leq \vartheta_{k+1}(r_i),$$

and for $i = \mathcal{N}/2, ..., \mathcal{N}$ apply the Lemma 6.6 we get the result

$$\Big|\mathcal{B}_{k+1}(r_i) - \hat{\mathcal{B}}^{\mathcal{N}}_{k+1}(r_i)\Big| \leq \mathcal{C}\max\{\mathcal{N}^{-2}, \mathcal{N}^{-5+4i/\mathcal{N}\ln\mathcal{N}}\}. \tag{6.9}$$

Now, we combined the Equations (6.7) and (6.9) and obtained the required results. □

Theorem 6.9. *The error in the solution $Y^{\mathcal{N}}_{k+1}$ satisfies the following estimate*

$$\Big|y_{k+1}(r_i) - Y^{\mathcal{N}}_{k+1}(r_i)\Big| \leq \begin{cases} \mathcal{C}\mathcal{N}^{-1}(\varepsilon + \mathcal{N}^{-1}), & \textit{for} \quad 0 \leq i < \mathcal{N}/2, \\ \mathcal{C}\mathcal{N}^{-1}\Big(\varepsilon + \mathcal{N}^{-4(1-i/\mathcal{N})\ln\mathcal{N}}\Big), & \textit{for} \quad \mathcal{N}/2 \leq i \leq \mathcal{N}. \end{cases} \tag{6.10}$$

Proof. The combined result is derived by merging the error estimates provided by Theorem 6.7 for the smooth component and those given by Theorem 6.8 for the singular component. □

Theorem 6.10. *Suppose that $y(r,\theta)$ be the solution of the Equation (2.1) and $y_{k+1}(r)$ be the solution of discrete problem (3.1) also $Y^{\mathcal{N}}_{k+1}$ be the solution of the Equation (5.13), satisfying the following error estimate*

$$\Big|\Big|y_{k+1}(r_i,\theta_{k+1}) - Y^{\mathcal{N}}_{k+1}(r_i)\Big|\Big| \leq \begin{cases} \mathcal{C}\Delta\theta + \mathcal{C}\mathcal{N}^{-1}(\varepsilon + \mathcal{N}^{-1}), & \textit{for} \quad 0 \leq i < \mathcal{N}/2, \\ \mathcal{C}\Delta\theta + \mathcal{C}\mathcal{N}^{-1}\Big(\varepsilon + \mathcal{N}^{-4(1-i/\mathcal{N})\ln\mathcal{N}}\Big), & \textit{for} \quad \mathcal{N}/2 \leq i \leq \mathcal{N}. \end{cases} \tag{6.11}$$

Proof. We have the error inequality from the Equation (6.11) such that

$$\begin{aligned}\Big|\Big|y_{k+1}(r_i,\theta_{k+1}) - Y^{\mathcal{N}}_{k+1}(r_i)\Big|\Big| &= \Big|\Big|y_{k+1}(r_i,\theta_{k+1}) - y_{k+1}(r_i) + y_{k+1}(r_i) - Y^{\mathcal{N}}_{k+1}(r_i)\Big|\Big|, \\ &\leq \Big|\Big|y_{k+1}(r_i,\theta_{k+1}) - y_{k+1}(r_i)\Big|\Big| + \Big|\Big|y_{k+1}(r_i) - Y^{\mathcal{N}}_{k+1}(r_i)\Big|\Big|,\end{aligned}$$

Now, we used the Theorems 3.3 and 6.9 obtained the required result

$$\Big|\Big|y_{k+1}(r_i,\theta_{k+1}) - Y^{\mathcal{N}}_{k+1}(r_i)\Big|\Big| \leq \begin{cases} \mathcal{C}\Delta\theta + \mathcal{C}\mathcal{N}^{-1}(\varepsilon + \mathcal{N}^{-1}), & \text{for} \quad 0 \leq i < \mathcal{N}/2, \\ \mathcal{C}\Delta\theta + \mathcal{C}\mathcal{N}^{-1}\Big(\varepsilon + \mathcal{N}^{-4(1-i/\mathcal{N})\ln\mathcal{N}}\Big), & \text{for} \quad \mathcal{N}/2 \leq i \leq \mathcal{N}. \end{cases}$$

□

7. Examples and their numerical results

In this section, we will study two problems to validate the theoretical results established. The first problem considered is with the exact solution whereas the second problem does not have closed-form of exact solution. The double mesh principle is adopted for calculating order of convergence where the problem does not have exact solution.

Example 7.1. Consider the following parabolic initial-boundary value problem:

$$\begin{cases} y_\theta - \varepsilon y_{rr} + \Big(1 + r(1-r)\Big) y_r = f(r,\theta), \quad (r,\theta) \in (0,1) \times (0,1], \\ y(r,0) = y_0(r), \quad 0 < r < 1, \\ y(0,\theta) = 0, \quad y(1,\theta) = 0, \quad 0 \le \theta \le 1. \end{cases} \tag{7.1}$$

We choose the initial data $y_0(r)$ and the source function $f(r,\theta)$ to fit with the exact solution

$$y(r,\theta) = e^{-\theta}(\mathcal{C}_1 + \mathcal{C}_2 r - e^{-(1-r)/\varepsilon}),$$

where $\mathcal{C}_1 = e^{-1/\varepsilon}$ and $\mathcal{C}_2 = 1 - e^{-1/\varepsilon}$. As the exact solution of the Example 7.1 is known, for each ε , we calculate the maximum point-wise error by

$$E_\varepsilon^{\mathcal{N},\Delta\theta} = \max_{(r_i^k,\theta_k)\in \overline{G}_\varepsilon^{\mathcal{M},\mathcal{N}}} |y(r_i^k,\theta_k) - Y^{\mathcal{N},\Delta\theta}(r_i^k,\theta_k)|,$$

where $y(r_i^k,\theta_k)$ and $Y^{\mathcal{N},\Delta\theta}(r_i^k,\theta_k)$ respectively, denote the exact and the numerical solution obtained on the mesh with $\mathcal{N}$ mesh intervals in the spatial direction and $\mathcal{M}$ mesh intervals in the θ-direction such that $\Delta\theta = \mathcal{T}/\mathcal{M}$ is the uniform time step. In addition, we determine the corresponding order of convergence by

$$R_\varepsilon^{\mathcal{N},\Delta\theta} = \log_2\left(\frac{E_\varepsilon^{\mathcal{N},\Delta\theta}}{E_\varepsilon^{2\mathcal{N},\Delta\theta/2}}\right).$$

Now, for each $\mathcal{N}$ and $\Delta\theta$, we define $E^{\mathcal{N},\Delta\theta} = \max_\varepsilon E_\varepsilon^{\mathcal{N},\Delta\theta}$ as the ε-uniform maximum point-wise error and the corresponding local ε-uniform order of convergence is defined by

$$R^{\mathcal{N},\Delta\theta} = \log_2\left(\frac{E_\varepsilon^{\mathcal{N},\Delta\theta}}{E^{2\mathcal{N},\Delta\theta/2}}\right).$$

The calculated maximum point-wise errors $E_\varepsilon^{\mathcal{N},\Delta\theta/2}$ and the corresponding order of convergence $R_\varepsilon^{\mathcal{N},\Delta\theta}$ for Example 7.1 are presented in Tables 1, 3, and 5 for various values of ε and $\mathcal{N}$. From these results, one can observe the ε-uniform Second-order convergence of the numerical solution.

Example 7.2. Consider the following parabolic initial-boundary value problem:

$$\begin{cases} y_\theta - \varepsilon y_{rr} + \left(1 + r^2 + \dfrac{sin(\pi r)}{2}\right) y_r + (1 + r^2 + \dfrac{1}{2} sin(\pi\theta/2))y = f(r,\theta), \\ f(r,\theta) = r^3(1-r)^3\theta(1-\theta)sin(\pi\theta), \quad \text{for} \quad (r,\theta) \in (0,1)\times(0,1), \\ y(r,0) = 0, \ 0 < r < 1, \\ y(0,\theta) = y(1,\theta) = 0, \ 0 \le r \le 1. \end{cases} \tag{7.2}$$

As the exact solution of problem 7.2 is not known, to obtain the accuracy of the numerical solution and also to demonstrate the ε-uniform convergence of the proposed scheme, we use the double mesh principle which is given in the following. Let $\tilde{Y}^{2\mathcal{N},\Delta\theta/2}(r_i^k,\theta_k)$ be the numerical solution obtained on the proposed mesh with $2\mathcal{N}$ mesh intervals in spatial direction and $2\mathcal{M}$ mesh intervals in the θ-direction. Then, for each ε we calculate the maximum point-wise error by

$$E_\varepsilon^{\mathcal{N},\Delta\theta} = \max_{(r_i^k,\theta_k)\in \overline{G}_\varepsilon^{\mathcal{M},\mathcal{N}}} |Y^{\mathcal{N},\Delta\theta}(r_i^k,\theta_k) - \tilde{Y}^{2\mathcal{N},\Delta\theta/2}(r_i^k,\theta_k)|,$$

and the corresponding order of convergence by

$$R_\varepsilon^{\mathcal{N},\Delta\theta} = \log_2\left(\frac{E_\varepsilon^{\mathcal{N},\Delta\theta}}{E_\varepsilon^{2\mathcal{N},\Delta\theta/2}}\right).$$

The calculated maximum point-wise errors $E_\varepsilon^{\mathcal{N},\Delta\theta}$ and the corresponding order of convergence $R_\varepsilon^{\mathcal{N},\Delta\theta}$ for Example 7.2 are given in Tables 2, 4, and 6, respectively. The numerical results given in these tables reveal the Second-order convergence independent of the diffusion parameter ε. The maximum point-wise errors are plotted in log-log scale in

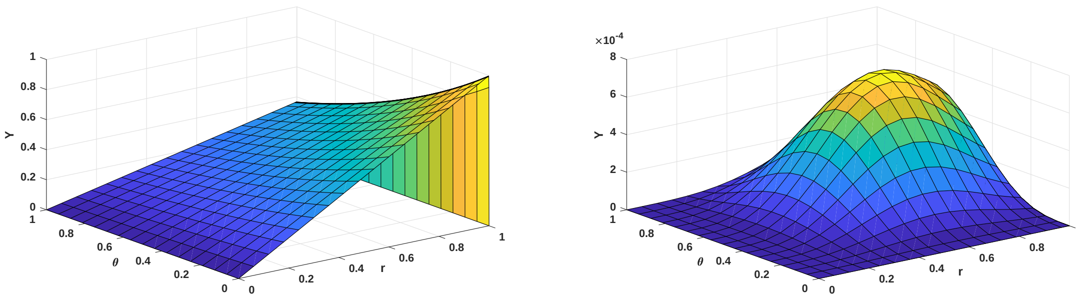

(a) $\mathcal{N} = 32, \mathcal{M} = 16, \varepsilon = 2^{-12}$.

(b) $\mathcal{N} = 32, \mathcal{M} = 16, \varepsilon = 2^{-12}$.

FIGURE 1. Solution profile for Example 7.1 and Example 7.2 in Figure 1(a) and 1(b) of the mesh (5.2).

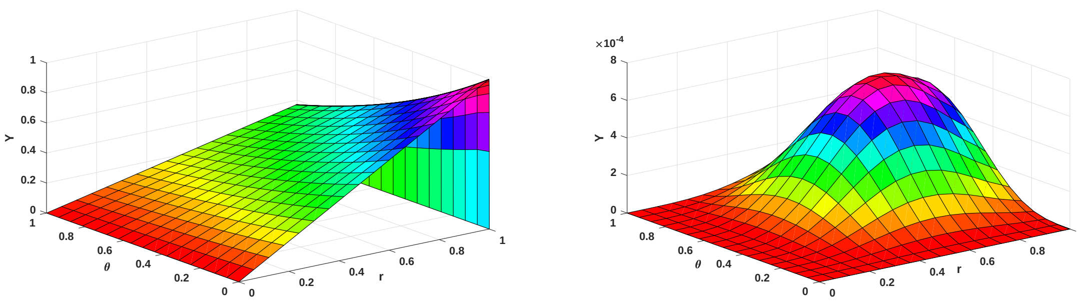

(a) $\mathcal{N} = 32, \mathcal{M} = 16, \varepsilon = 2^{-12}$.

(b) $\mathcal{N} = 32, \mathcal{M} = 16, \varepsilon = 2^{-12}$.

FIGURE 2. Solution profile for Examples 7.1 and 7.2 in Figures 2(a) and 2(b) of the mesh (5.3).

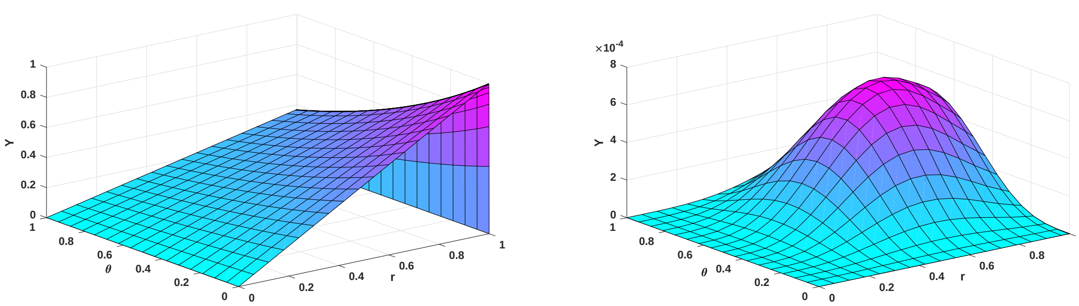

(a) $\mathcal{N} = 32, \mathcal{M} = 16, \varepsilon = 2^{-12}$.

(b) $\mathcal{N} = 32, \mathcal{M} = 16, \varepsilon = 2^{-12}$.

FIGURE 3. Solution profile for Examples 7.1 and 7.2 in Figures 3(a) and 3(b) of the mesh (5.4).

Figures 4, 5, and 6, for the solution. From these figures, one can easily observe the Second-order ε-uniform convergence. The numerical solution is plotted in Figures 1, 2, and 3 for ε^{-12}. These figures show the existence of the boundary layer near $r = 0$.

Table 1. Maximum point-wise errors $E_{\varepsilon}^{\mathcal{N},\Delta\theta}$ and order of convergence of the solution $R_{\varepsilon}^{\mathcal{N},\Delta\theta}$ for Example 7.1 on Shishkin mesh using midpoint finite difference scheme.

	Number of Intervals $\mathcal{N},\mathcal{M}$				
	$\mathcal{N}=84$	$\mathcal{N}=168$	$\mathcal{N}=336$	$\mathcal{N}=672$	$\mathcal{N}=1344$
ε	$\mathcal{M}=5$	$\mathcal{M}=20$	$\mathcal{M}=80$	$\mathcal{M}=320$	$\mathcal{M}=1280$
2^{-12}	$5.4953e-02$	$1.6291e-02$	$5.2358e-03$	$1.6496e-03$	$5.0544e-04$
	1.7541	1.6376	1.6663	1.7065	
2^{-15}	$5.5048e-02$	$1.6386e-02$	$5.2450e-03$	$1.6538e-03$	$5.0654e-04$
	1.7483	1.6434	1.6651	1.7071	
2^{-18}	$5.5060e-02$	$1.6397e-02$	$5.2609e-03$	$1.6542e-03$	$5.0686e-04$
	1.7475	1.6401	1.6691	1.7065	
2^{-21}	$5.5061e-02$	$1.6399e-02$	$5.2629e-03$	$1.6561e-03$	$5.0690e-04$
	1.7474	1.6397	1.6680	1.7080	
2^{-24}	$5.5061e-02$	$1.6399e-02$	$5.2631e-03$	$1.6565e-03$	$5.0704e-04$
	1.7474	1.6396	1.6678	1.7079	
$E^{\mathcal{N},\Delta\theta}$	$5.6061e-02$	$1.7399e-02$	$5.3631e-03$	$1.7565e-03$	$5.1704e-04$
$R^{\mathcal{N},\Delta\theta}$	1.7674	1.7396	1.8678	1.8079	

Table 2. Maximum point-wise errors $E_{\varepsilon}^{\mathcal{N},\Delta\theta}$ and order of convergence of the solution $R_{\varepsilon}^{\mathcal{N},\Delta\theta}$ for Example 7.2 on Shishkin mesh using midpoint finite difference scheme.

	Number of Intervals $\mathcal{N},\mathcal{M}$				
	$\mathcal{N}=84$	$\mathcal{N}=168$	$\mathcal{N}=336$	$\mathcal{N}=672$	$\mathcal{N}=1344$
ε	$\mathcal{M}=5$	$\mathcal{M}=20$	$\mathcal{M}=80$	$\mathcal{M}=320$	$\mathcal{M}=1280$
2^{-12}	$1.2751e-04$	$4.1774e-05$	$1.1382e-05$	$2.9000e-06$	$7.2852e-07$
	1.6100	1.8759	1.9726	1.9930	
2^{-15}	$1.2757e-04$	$4.1821e-05$	$1.1394e-05$	$2.9030e-06$	$7.2920e-07$
	1.6090	1.8759	1.9727	1.9932	
2^{-18}	$1.2758e-04$	$4.1827e-05$	$1.1396e-05$	$2.9034e-06$	$7.2936e-07$
	1.6089	1.8759	1.9727	1.9931	
2^{-21}	$1.2758e-04$	$4.1828e-05$	$1.1396e-05$	$2.9035e-06$	$7.2938e-07$
	1.6089	1.8759	1.9727	1.9931	
2^{-24}	$1.2758e-04$	$4.1828e-05$	$1.1396e-05$	$2.9035e-06$	$7.2939e-07$
	1.6089	1.8759	1.9727	1.9931	
$E^{\mathcal{N},\Delta\theta}$	$1.2758e-04$	$4.1828e-05$	$1.1396e-05$	$2.9035e-06$	$7.2939e-07$
$R^{\mathcal{N},\Delta\theta}$	1.6089	1.8759	1.9727	1.9931	

Table 3. Maximum point-wise errors $E_{\varepsilon}^{\mathcal{N},\Delta\theta}$ and order of convergence of the solution $R_{\varepsilon}^{\mathcal{N},\Delta\theta}$ for Example 7.1 on Shishkin-Bakhvalov mesh using midpoint finite difference scheme.

	Number of Intervals $\mathcal{N},\mathcal{M}$				
	$\mathcal{N}=84$	$\mathcal{N}=168$	$\mathcal{N}=336$	$\mathcal{N}=672$	$\mathcal{N}=1344$
ε	$\mathcal{M}=5$	$\mathcal{M}=20$	$\mathcal{M}=80$	$\mathcal{M}=320$	$\mathcal{M}=1280$
2^{-12}	$1.7670e-02$	$4.9931e-03$	$1.2944e-03$	$3.2668e-04$	$8.1865e-05$
	1.8233	1.9476	1.9864	1.9965	
2^{-15}	$1.7696e-02$	$5.0000e-03$	$1.2962e-03$	$3.2713e-04$	$8.1979e-05$
	1.8234	1.9476	1.9864	1.9965	
2^{-18}	$1.7699e-02$	$5.0009e-03$	$1.2965e-03$	$3.2719e-04$	$8.1993e-05$
	1.8234	1.9476	1.9864	1.9965	
2^{-21}	$1.7700e-02$	$5.0010e-03$	$1.2965e-03$	$3.2720e-04$	$8.1995e-05$
	1.8234	1.9476	1.9864	1.9965	
2^{-24}	$1.7700e-02$	$5.0010e-03$	$1.2965e-03$	$3.2720e-04$	$8.1995e-05$
	1.8234	1.9476	1.9864	1.9965	
$E^{\mathcal{N},\Delta\theta}$	$1.7500e-02$	$5.1010e-03$	$1.2965e-03$	$3.3720e-04$	$8.0995e-05$
$R^{\mathcal{N},\Delta\theta}$	1.7834	1.9576	1.9464	1.9965	

Table 4. Maximum point-wise errors $E_{\varepsilon}^{\mathcal{N},\Delta\theta}$ and order of convergence of the solution $R_{\varepsilon}^{\mathcal{N},\Delta\theta}$ for Example 7.2 on Shishkin-Bakhvalov mesh using midpoint finite difference scheme.

	Number of Intervals $\mathcal{N},\mathcal{M}$				
	$\mathcal{N}=84$	$\mathcal{N}=168$	$\mathcal{N}=336$	$\mathcal{N}=672$	$\mathcal{N}=1344$
ε	$\mathcal{M}=5$	$\mathcal{M}=20$	$\mathcal{M}=80$	$\mathcal{M}=320$	$\mathcal{M}=1280$
2^{-12}	$1.2751e-04$	$4.1781e-05$	$1.1382e-05$	$2.8997e-06$	$7.2835e-07$
	1.6097	1.8761	1.9728	1.9932	
2^{-15}	$1.2757e-04$	$4.1827e-05$	$1.1395e-05$	$2.9030e-06$	$7.2907e-07$
	1.6088	1.8760	1.9728	1.9934	
2^{-18}	$1.2758e-04$	$4.1833e-05$	$1.1397e-05$	$2.9035e-06$	$7.2922e-07$
	1.6087	1.8760	1.9727	1.9934	
2^{-21}	$1.2758e-04$	$4.1834e-05$	$1.1397e-05$	$2.9036e-06$	$7.2925e-07$
	1.6087	1.8760	1.9727	1.9934	
2^{-24}	$1.2758e-04$	$4.1834e-05$	$1.1397e-05$	$2.9036e-06$	$7.2925e-07$
	1.6087	1.8760	1.9727	1.9934	
$E^{\mathcal{N},\Delta\theta}$	$1.3758e-04$	$4.1534e-05$	$1.2397e-05$	$2.9136e-06$	$7.2915e-07$
$R^{\mathcal{N},\Delta\theta}$	1.7087	1.8860	1.9727	1.9934	

TABLE 5. Maximum point-wise errors $E_\varepsilon^{\mathcal{N},\Delta\theta}$ and order of convergence of the solution $R_\varepsilon^{\mathcal{N},\Delta\theta}$ for Example 7.1 on Shishkin-Bakhvalov modified mesh using midpoint finite difference scheme.

	Number of Intervals $\mathcal{N},\mathcal{M}$				
	$\mathcal{N}=84$	$\mathcal{N}=168$	$\mathcal{N}=336$	$\mathcal{N}=672$	$\mathcal{N}=1344$
ε	$\mathcal{M}=5$	$\mathcal{M}=20$	$\mathcal{M}=80$	$\mathcal{M}=320$	$\mathcal{M}=1280$
2^{-12}	$1.7663e-02$	$4.9935e-03$	$1.2951e-03$	$3.2697e-04$	$8.1966e-05$
	1.8226	1.9470	1.9859	1.9961	
2^{-15}	$1.7690e-02$	$5.0007e-03$	$1.2970e-03$	$3.2743e-04$	$8.2080e-05$
	1.8227	1.9470	1.9859	1.9961	
2^{-18}	$1.7693e-02$	$5.0017e-03$	$1.2972e-03$	$3.2749e-04$	$8.2094e-05$
	1.8227	1.9470	1.9859	1.9961	
2^{-21}	$1.7694e-02$	$5.0018e-03$	$1.2972e-03$	$3.2750e-04$	$8.2096e-05$
	1.8227	1.9470	1.9859	1.9961	
2^{-24}	$1.7694e-02$	$5.0018e-03$	$1.2972e-03$	$3.2750e-04$	$8.2096e-05$
	1.8227	1.9470	1.9859	1.9961	
$E^{\mathcal{N},\Delta\theta}$	$1.7794e-02$	$5.1018e-03$	$1.3972e-03$	$3.3750e-04$	$8.3096e-05$
$R^{\mathcal{N},\Delta\theta}$	1.8327	1.9570	1.9759	1.9861	

TABLE 6. Maximum point-wise errors $E_\varepsilon^{\mathcal{N},\Delta\theta}$ and order of convergence of the solution $R_\varepsilon^{\mathcal{N},\Delta\theta}$ for Example 7.2 on Shishkin-Bakhvalov modified mesh using midpoint finite difference scheme.

	Number of Intervals $\mathcal{N},\mathcal{M}$				
	$\mathcal{N}=84$	$\mathcal{N}=168$	$\mathcal{N}=336$	$\mathcal{N}=672$	$\mathcal{N}=1344$
ε	$\mathcal{M}=5$	$\mathcal{M}=20$	$\mathcal{M}=80$	$\mathcal{M}=320$	$\mathcal{M}=1280$
2^{-12}	$1.2751e-04$	$4.1775e-05$	$1.1381e-05$	$2.8997e-06$	$7.2846e-07$
	1.6099	1.8760	1.9727	1.9930	
2^{-15}	$1.2757e-04$	$4.1822e-05$	$1.1394e-05$	$2.9030e-06$	$7.2918e-07$
	1.6090	1.8760	1.9727	1.9932	
2^{-18}	$1.2758e-04$	$4.1828e-05$	$1.1396e-05$	$2.9035e-06$	$7.2936e-07$
	1.6089	1.8759	1.9727	1.9931	
2^{-21}	$1.2758e-04$	$4.1828e-05$	$1.1396e-05$	$2.9035e-06$	$7.2938e-07$
	1.6089	1.8759	1.9727	1.9931	
2^{-24}	$1.2758e-04$	$4.1829e-05$	$1.1396e-05$	$2.9035e-06$	$7.2938e-07$
	1.6089	1.8759	1.9727	1.9931	
$E^{\mathcal{N},\Delta\theta}$	$1.2758e-04$	$4.1829e-05$	$1.1396e-05$	$2.9035e-06$	$7.2938e-07$
$R^{\mathcal{N},\Delta\theta}$	1.6089	1.8759	1.9727	1.9931	

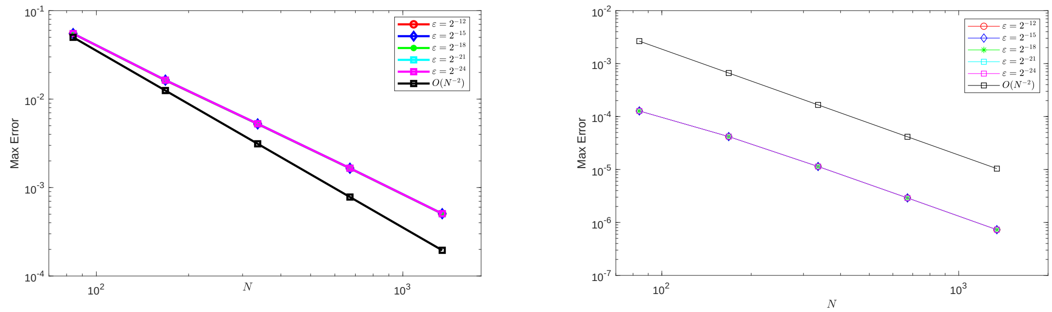

(a) $\mathcal{N}$ is doubled but $\mathcal{M}$ is quadrupled.

(b) $\mathcal{N}$ is doubled but $\mathcal{M}$ is quadrupled.

FIGURE 4. Loglog plot for Examples 7.1 and 7.2 in Figures 4(a) and 4(b) of the mesh in Equation (5.2) for values of $\mathcal{N}$ and $\mathcal{M}$ where grids point $\mathcal{N}$ is doubled but $\mathcal{M}$ is quadrupled and $\varepsilon = \{2^{-12}, 2^{-15}, 2^{-18}, 2^{-21}, 2^{-24}\}$.

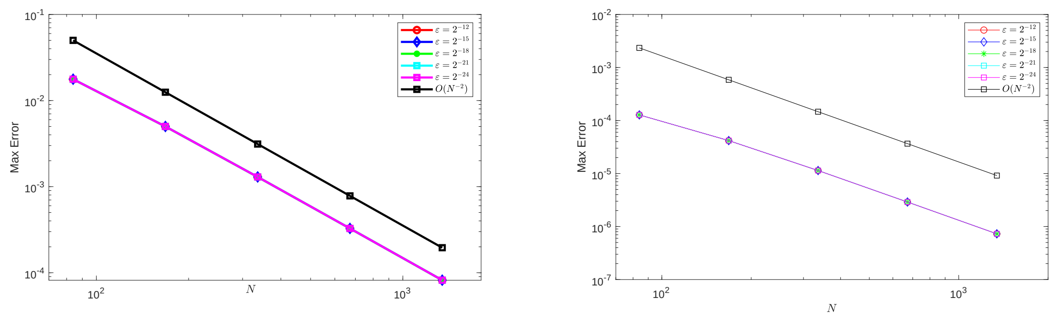

(a) $\mathcal{N}$ is doubled but $\mathcal{M}$ is quadrupled.

(b) $\mathcal{N}$ is doubled but $\mathcal{M}$ is quadrupled.

FIGURE 5. Loglog plot for Examples 7.1 and 7.2 in Figures 5(a) and 5(b) of the mesh in Equation (5.3) for values of $\mathcal{N}$ and $\mathcal{M}$ where grids point $\mathcal{N}$ is doubled but $\mathcal{M}$ is quadrupled and $\varepsilon = \{2^{-12}, 2^{-15}, 2^{-18}, 2^{-21}, 2^{-24}\}$.

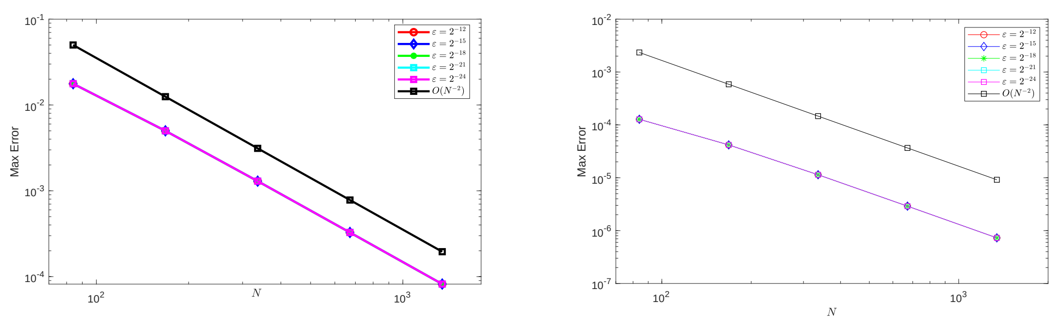

(a) $\mathcal{N}$ is doubled but $\mathcal{M}$ is quadrupled.

(b) $\mathcal{N}$ is doubled but $\mathcal{M}$ is quadrupled.

FIGURE 6. Loglog plot for Examples 7.1 and 7.2 in Figures 6(a) and 6(b) of the mesh in Equation (5.4) for values of $\mathcal{N}$ and $\mathcal{M}$ where grids point $\mathcal{N}$ is doubled but $\mathcal{M}$ is quadrupled and $\varepsilon = \{2^{-12}, 2^{-15}, 2^{-18}, 2^{-21}, 2^{-24}\}$.

8. Conclusion

In this study, we introduces numerical approached for solving a singularly perturbed time-dependent convection-diffusion problem featuring a boundary layer on the right side of the domain. The proposed method involves employing Euler discretization in the time direction and midpoint-upwind discretization in the spatial direction with the mesh type are classical Shishkin mesh, Shishkin-Bakhvalov mesh, and Shishkin-Bakhvalov modified mesh. We demonstrate the method's accuracy, showing it to be first-order accurate in the time and achieving the second-order accuracy in space on a coarse part of the domain and upto the second order accuracy on fine part of the domain. Extensive analysis has been conducted to derive uniform error estimates for both coarse and fine parts. In support of the predicted theory, two test examples were examined using the proposed methods, resulting in numerical results. The performance of the method is illustrated through maximum point-wise errors presented in Tables 1–6, while computed solutions are visualized in Figures 1–3. These graphs and tables depict the physical behaviour of the computed solutions. Also the errors in Tables 1-6, indicate that the proposed method achieves uniform convergence with respect to the perturbation parameter, which confirms the theoretical results established.

Data Availability:

Enquiries about data availability should be directed to the authors.

Conflict of interest:

The authors declare that they have no conflict of interest.

References

[1] N. Aghazadeh, K. Rabbani, S. H. T. Otaghsara, and M. Rabbani, *A finite difference approach to solve the nonlinear model of electro-osmotic flow in nano-channels*, Comput. Methods Differ. Equ., *13*(3) (2025).

[2] M. P. Alam, G. Manchanda, and A. Khan, *An ε-uniformly convergent method for singularly perturbed parabolic problems exhibiting boundary layers*, J. Appl. Anal. Comput., *13*(4) (2023), 2089–2120.

[3] M. A. Ayele, A. A. Tiruneh, and G. A. Derese, *Hybrid fitted numerical scheme for singularly perturbed convection-diffusion problem with a small time lag*, Wiley Online Library, *2023*(1) (2023), 1–15 .

[4] L. Bobisud, *Second-order linear parabolic equations with a small parameter*, Arch. Ration. Mech. Anal., *27*(5) (1968), 385–397.

[5] C. Clavero, J. L. Gracia, and M. Stynes, *A simpler analysis of a hybrid numerical method for time-dependent convection–diffusion problems*, J. Comput. Appl. Math., *235*(17) (2011), 5240–5248.

[6] G. F. Duressa, F. W. Gelu, and G. D. Kebede, *A robust higher-order fitted mesh numerical method for solving singularly perturbed parabolic reaction-diffusion problems*, Res. Appl. Math., *20* (2023), 100405.

[7] P. Farrell, A. Hegarty, J. M. Miller, E. O'Riordan, and G. I. Shishkin, *Robust computational techniques for boundary layers*, Chapman and hall/CRC, (2000).

[8] A. Fröhner, T. Linß, and H. G. Roos, *Defect correction on shishkin-type meshes*, Numerical Algorithms, *26* (2001), 281–299.

[9] F. W. Gelu and G. F. Duressa, *Hybrid method for singularly perturbed robin type parabolic convection–diffusion problems on shishkin mesh*, PDE Appl. Math., *8* (2023), 100586.

[10] F. W. Gelu and G. F. Duressa, *A parameter-uniform numerical method for singularly perturbed robin type parabolic convection-diffusion turning point problems*, Appl. Numer. Math., *190* (2023), 50–64.

[11] W. T. Gobena and G. F. Duressa, *Exponentially fitted robust scheme for the solution of singularly perturbed delay parabolic differential equations with integral boundary condition*, Int. J. Appl. Comput. Math., *10*(1) (2024), 1–21.

[12] P. Hemker, G. I. Shishkin, and L. P. Shishkina, *ε-uniform schemes with high-order time-accuracy for parabolic singular perturbation problems*, IMA J. Numer. Anal., *20*(1) (2000), 99–121.

[13] M. K. Kadalbajoo and A. Awasthi, *The midpoint upwind finite difference scheme for time-dependent singularly perturbed convection-diffusion equations on non-uniform mesh*, Int. J. Comput. Methods Eng. Sci. Mech., *12*(3) (2011), 150–159.

[14] R. B. Kellogg and A. Tsan, *Analysis of some difference approximations for a singular perturbation problem without turning points*, Mathematics of computation, *32*(144) (1978), 1025–1039.

[15] H. G. Lee, S. Ham, and J. Kim, *Isotropic finite difference discrettization of laplacian operator*, Appl. Comput. Math, *22*(2) (2023), 259–274.

[16] T. Linß, *An upwind difference scheme on a novel shishkin-type mesh for a linear convection–diffusion problem*, J. Comput. Appl. Math., *110*(1) (1999), 93–104.

[17] W. S. Manebo, M. M. Woldaregay, T. G. Dinka, and G. F. Duressa, *An equidistributed grid-based second-order scheme for a singularly perturbed fredholm integro-differential equation with an interior, layer*, Appl. Math. Comput., *464* (2024), 128398.

[18] J. J. Miller, E. O'riordan, and G. I. Shishkin, *Fitted numerical methods for singular perturbation problems:error estimates in the maximum norm for linear problems in one and two dimensions*, World scientific, (1996).

[19] K. Mukherjee and S. Natesan, *Parameter-uniform hybrid numerical scheme for time-dependent convection-dominated initial-boundary-value problems*, Computing, *84* (2009), 209–230.

[20] H. G. Roos, *Robust numerical methods for singularly perturbed differential equations*, Springer, (2008).

[21] K. K. Sah and S. Gowrisankar, *Richardson extrapolation technique on a modified graded mesh for singularly perturbed parabolic convection-diffusion problems*, Iran. J. Numer. Anal. Optim., *14*(1) (2024), 219–264.

[22] M. Stynes and E. O'Riordan, *Uniformly convergent difference schemes for singularly perturbed parabolic diffusion-convection problems without turning points*, Numerische Mathematik, *55*(5) (1989),521–544.

[23] M. Stynes and H. G. Roos, *The midpoint upwind scheme*, Applied Numerical Mathematics, *23*(3) (1997), 361–374.

[24] S. Tian, X. Liu, and R. An, *A higher-order finite difference scheme for singularly perturbed parabolic problem*, Math. Probl. Eng., *2021*(1) (2021), 1–11.

[25] G. M. Wondimu, G. F. Duressa, M. M. Woldaregay, and T. G. Dinka, *A uniformly convergent computational method for singularly perturbed parabolic partial differential equation with integral boundary condition.*, J. Math. Model., *12*(1) (2024), 157–175.

[26] S. W. Worku and G. F. Duressa, *A numerical approach for diffusion-dominant two-parameter singularly perturbed delay parabolic differential equations*, Int. J. Math. Math. Sci., *2023*(1) (2023), 1–17.

[27] H. Xu, M. Khalsaraei, A. Shokri, H. Ramos, and M. Molayi, *Nonstandard finite difference schemes with positivity property with application to a mathematical model of hiv infection*, Appl. Comput. Math., *23*(4) (2024), 541–557.